Evaluation of classical reinforcement and passive control systems on a reinforced concrete bridge subjected to seismic loading

Germán Nanclares, Daniel Ambrosini* and Oscar Curadelli

Engineering Faculty,
National University of Cuyo
Parque Gral. San Martín, Mendoza, Argentina
and
CONICET,
Av. Ruiz Leal, 5500 Mendoza, Argentina
Email: dambrosini@uncu.edu.ar
*Corresponding author

Abstract: In this paper, different strategies are studied with the main objective to reduce structural demand and damage of an existent bridge in Mendoza, Argentina, with post-tensioning reinforced concrete girders that are a common structural typology in the region. A numerical study was carried out with this purpose. The numerical model was calibrated against experimental measurements of vibration natural frequencies. The alternatives studied are: a) classical reinforcement of the structural overall stiffness; b) tuned mass dampers; c) viscous dampers; d) metallic dampers. The model is subjected to real near-fault seismic records, thereby obtaining response parameters to evaluate the efficiency of each protective system. The response is evaluated not only in terms of reduction of displacements, but also in increasing of shear force in key elements, which is a negative characteristic of some of the systems studied. Advantages and disadvantages of each studied system are highlighted.

Keywords: control of vibration; passive systems; reinforced concrete bridge; numerical analysis; finite element modelling; experimental tests.

Reference to this paper should be made as follows: Nanclares, G., Ambrosini, D. and Curadelli, O. (2018) 'Evaluation of classical reinforcement and passive control systems on a reinforced concrete bridge subjected to seismic loading', *Int. J. Lifecycle Performance Engineering*, Vol. 2, Nos. 3/4, pp.189–209.

Biographical notes: Germán Nanclares obtained a degree in Civil Engineering (2011) at the National University of Cuyo, Argentina and received his MSc (2017) from the same university. He is a PhD student in the University of Cuyo and he has benefited a full scholarship from CONICET (Argentina) to finance his doctoral studies.

Daniel Ambrosini is a Full Professor in the Engineering Faculty at University of Cuyo, Argentina, since 2003. He holds a degree in Civil Engineering (1986) from the same university and an MSc (1991) and DrEng (1994) in Structures Institute at University of Tucuman, Argentina. He is a member of the National Academy of Engineering (Argentina), a Senior Researcher (CONICET, Argentina) and the Head of the Experimental Dynamics Division

(University of Cuyo). In 2001 and 2005, he was awarded from the National Academy of Engineering (Argentina) because his trajectory until 40 years and due to the better scientific contribution in 2005. His current research interests are structural dynamics, seismic, blast and wind loadings, control of vibration, structural damage and structural health monitoring (SHM).

Oscar Curadelli received his PhD in Engineering at the Federal University of Rio Grande do Sul, Brazil, in 2003, with a doctoral thesis entitled 'Structural vibration control by means of metallic dampers'. He is currently working as a Researcher at the CONICET and an Associate Professor at Engineering Faculty of National University of Cuyo, Argentina. His main research interest concerns vibration control.

1 Introduction

Road bridges are fundamental in the transport network and in the daily activity of populated regions. Therefore, their operating conditions after a major seismic event must remain unaltered in order to avoid the loss of human lives and to reduce economic issues associated with traffic disruption. Several authors have detailed seismic events where extensive damage, even total collapse, of road and railway bridges has occurred (Housner and Thiel, 1995; Kawashima and Unjoh, 1997; Hsu and Fu, 2004; Han et al., 2009; Kawashima et al., 2009, 2011). The causes of collapse have been found in shear failure in concrete columns, insufficient bearing support and steel reinforcement buckling, among others. It is known that excessive displacements lead to large internal forces with high level of associated damage, but it has also been demonstrated by several researchers, that vibration control systems are capable of improving seismic response of bridges and, thereby reduce damage of structural members (Agrawal et al., 2009).

Structural control systems are classified, according to their need for external energy supply to ensure its operation, into three main categories: active, semi-active and passive control systems. While active and semi-active protective systems require an external source of energy (Soong and Dargush, 1997), passive control systems use the energy coming from the movement of the structure itself (Beygi, 2015). In the last decades, semi-active control systems have been developed worldwide since they operate with lower energy than the active ones and take advantage of the benefits of both passive and active control systems in their performance (Soria et al., 2016). Despite the aforementioned features, passive systems continue to be an attractive solution in developing countries, owing to their low cost and maintenance.

On the other hand, it has also been demonstrated that isolation techniques perform better than passive systems, however this option, may be excessively expensive or technically more complex to solve when attempting to apply to existing structures. In this sense, passive control systems are not considered to be an alternative to seismic isolation, but rather an improvement on the structural safety of existing buildings (Domizio et al., 2015).

In this paper, different strategies are studied with the aim of reducing structural demand and damage of an existent bridge in Mendoza, Argentina, with post-tensioned reinforced concrete girders. A numerical study was carried out with this purpose.

The numerical model was calibrated against experimental measurements of natural frequencies of vibration. Only transversal seismic load is considered in analysis.

The alternatives studied are:

a classical reinforcement of the structural overall stiffness

b tuned mass dampers (TMDs)

c viscous dampers

d metallic dampers (MDs).

The model is subjected to real near-fault seismic records, thereby obtaining response parameters to evaluate the efficiency of each protective system. The response is evaluated not only in terms of reduction of displacements, but also in increasing of shear force in key elements, which is a negative characteristic of some of the systems studied. Advantages and disadvantages of each studied system are highlighted.

2 Structure descriptions

The structure studied is an existing bridge located in Mendoza, Argentina (Figure 1). It is a two-span bridge with post-tensioned RC girders and an intermediate support by means of a reinforced concrete frame that provides two independent structures of 29.25 m length each one. The middle frame is composed by three circular cross-section columns, 4.10 m height, jointed at the top by a robust rectangular beam. The road surface is a 50 mm thick asphalt layer, placed over a precast reinforced concrete deck. The aforementioned deck is discontinuous at the middle length, which is supported by six 'I' RC post-tensioned beams, separated 2.30 m, simply supported at each end. Both are connected by means of steel shear-key embedded into cast in-situ concrete.

Figure 1 Bridge studied (see online version for colours)

The major post-tensioned girders were built with 30 MPa strength concrete and the remaining structure with 21 MPa strength concrete. Elastomeric seat bearing was attached at both ends of each girder. The geometrics characteristics of the studied bridge are presented in Figure 2 and Figure 3.

Figure 2 Plan and longitudinal view of studied bridge (see online version for colours)

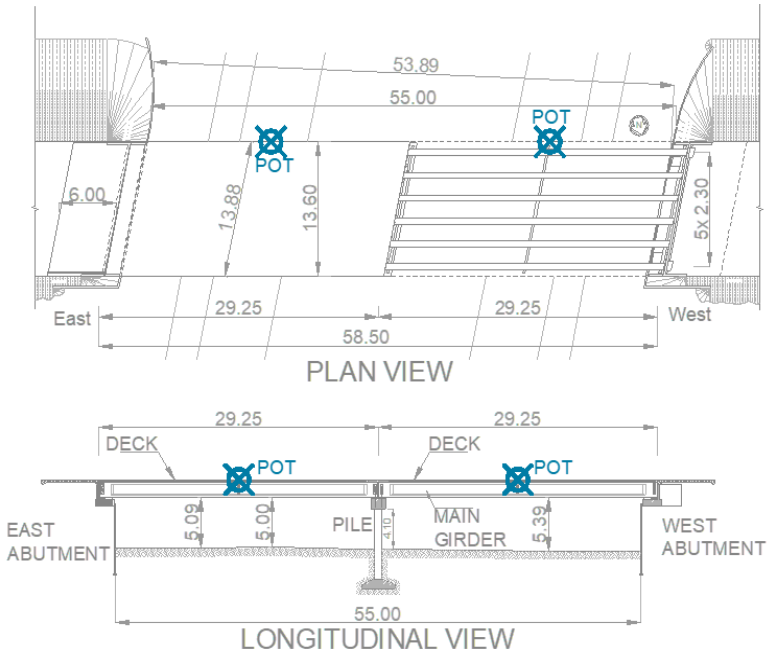

Note: Units in metres.

Figure 3 Transversal view of studied bridge (see online version for colours)

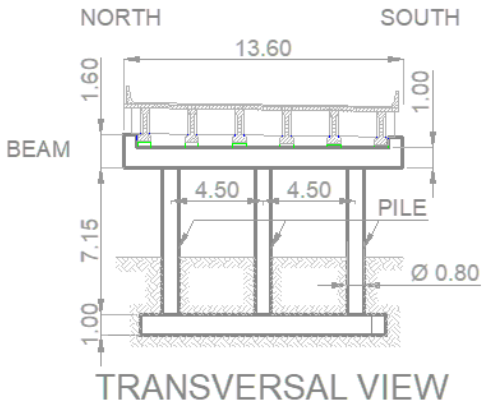

Notes: Pre-design, units in metres.

3 Experimental tests

With the aim of evaluating natural frequencies, a total of 14 horizontal and vertical time-acceleration records (seven on each side) lasting 100 seconds were measured on two points of testing (POT in Figure 2) under normal traffic. The acceleration time histories recorded are evaluated through fast Fourier transform (FFT), using the well

known peak-picking method to identify frequencies content. Figure 4 shows experimental results from the 8th test. A brief summary of the frequencies found in the experimental results is presented in Table 1.

Figure 4 Time histories records and Fourier spectra of 8th test, measured on the west side (see online version for colours)

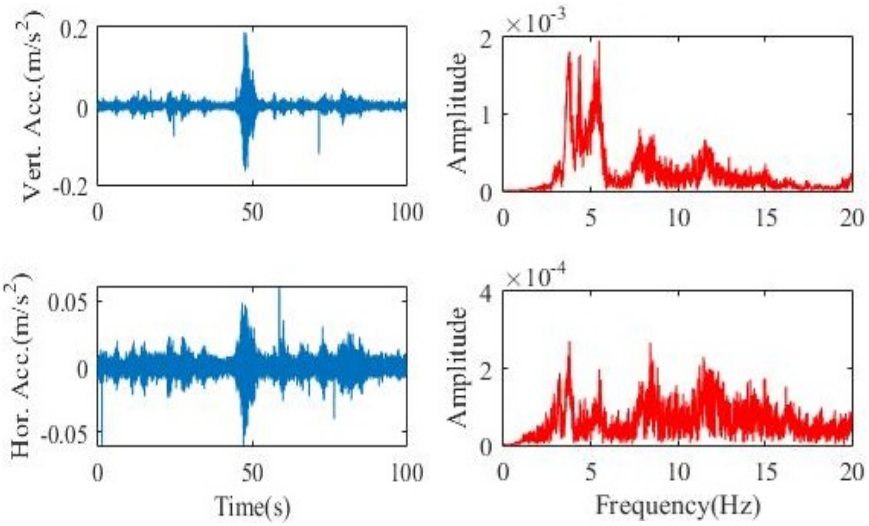

Table 1 Vibration frequencies and shapes from experimental tests

Mode	*Frequency [Hz]*	*Shape*
1	3.68	Lateral-torsional
2	4.24	Flexural vertical
3	5.47	Torsional

4 Modelling

4.1 Numerical model

The structure was modelled with ANSYS software (ANSYS Mechanical, 2010), using beam elements for the main structure (element type BEAM188, two-node with six degrees of freedom per node) and shell elements for the horizontal deck (SHELL181, four-node with six degrees of freedom each one). Connections between beams and shells are modelled as *bonded contact* including a vertical offset to consider the distance from the longitudinal axis of the girders to the axis of the deck. Regarding support of girders on the middle transverse frame, they are modelled as *joint connection* with rotational degrees of freedom released, by means of rigid link that are attached at the ends of the girders, in this way the elevation difference between both axes is taken into consideration. In relation of beam connections, they were considered as *joint connection*.

To model supports and rotational stiffness, linear spring elements were used (COMBIN14) both for the piles ends and for the major girders ends. An additional mass

of 105 kg/m^2 was incorporated in the model to take into consideration inertial effects produced by the asphaltic road surface. Linear-elastic behaviour of the structure is considered to the structure. The model was meshed accounting for 400 mm elements length, resulting in 4,078 total elements and 2,102 nodes (Figure 5). A proportional damping equal to 5% of critical is considered for the two first vibration modes (Clough and Penzien, 2003).

Figure 5 (a) Isometric view of the numerical model (b) Scheme of external constrains modelled (see online version for colours)

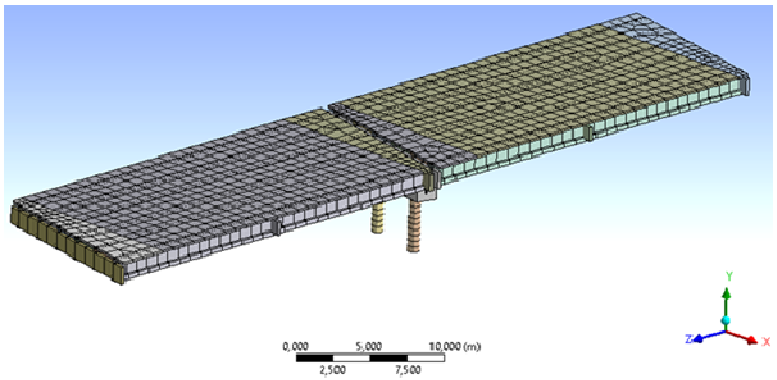

(a)

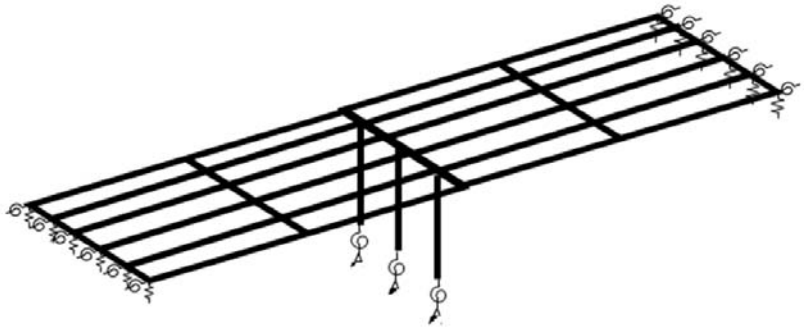

(b)

4.2 External loads

In addition to vertical forces originated by self-weight, horizontal seismic accelerations were considered from real earthquake records. The type of seismic acceleration records is 'near-fault', which are characterised by a short significant duration with a few pulses of high amplitude. Furthermore, its elastic response spectrum (Figure 6) indicates high incidence in the natural frequencies range of the bridge. The aforementioned seismic events are: Kobe, Japan earthquake in 1995 and Mendoza, Argentina earthquake in 1985 (Figure 6), Table 2 presents data related to the records.

Figure 6 Seismic records used and elastic response spectrum

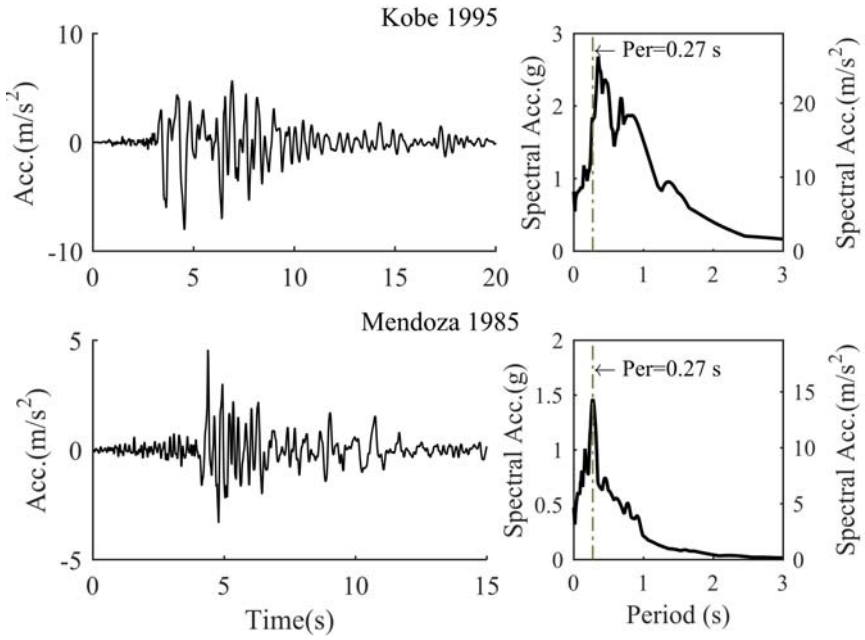

Note: 5% critical damping.

Table 2 Seismic records considered

Record	*Year*	*Station*	*PGA* [m/s^2]	*Moment magnitude*	*Failure dist. plane* [km]
Kobe	1995	KJMA	8.06	6.9	1.0
Mendoza	1985	-	4.57	6.3	-

Source: PEER Ground Motion Database [online] http://peer.berkeley.edu

The seismic acceleration was applied in transversal 'x' direction, from global coordinate system shown in Figure 5. This assumption is due to the collapse of highway bridges caused by lateral failure of intermediate support is a commonly observed case (Wotherspoon et al., 2011; Kawashima and Unjoh, 1997; Kawashima et al., 2009, 2011; Palermo et al., 2017).

4.3 Model calibrations

The stiffness of the springs was calibrated in such a way that frequencies obtained from a modal analysis coincide with experimentally measured values, shown in Table 3. It is worth noting that the second and third modes found in the numerical model are very close. For this reason, it was not possible distinguish between them in the experimental tests.

Table 3 Results obtained from modal analysis

Mode	*Numerical freq. (Hz)*	*Period (second)*	*Experimental freq. (Hz)*	*Diff. %*	*Modal shape*
1	3.68	0.27	3.68	0.0	Lateral torsional
2	4.22	0.24	4.24	0.5	Flexural vertical 1
3	4.26	0.24	--	--	Flexural vertical 2
4	5.45	0.18	5.47	0.4	Torsional

5 Structural response

The structural response from dynamic analysis in terms of: horizontal displacement of middle frame (u_x), shear force at the head of south column (V), horizontal support reaction (R_h) and vertical component of support reaction in south column bearing (R_v) are presented in Figure 7. Absolute maximum values are also included.

Figure 7 Numerical structural response

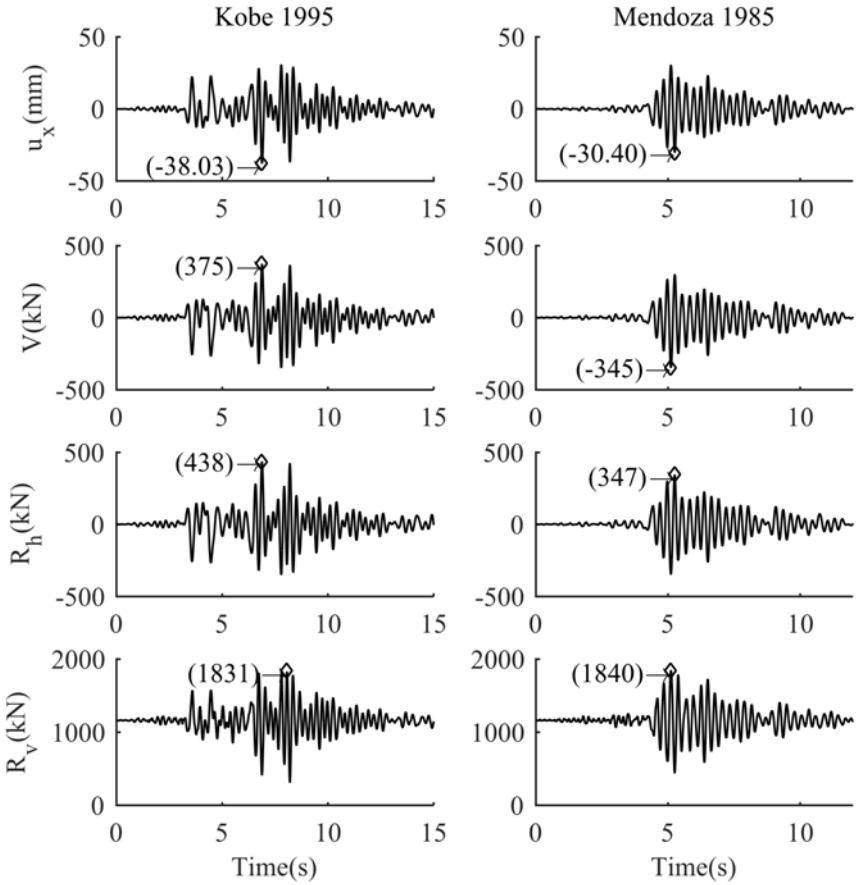

Note: Uncontrolled response.

6 Vibration control strategies

6.1 Reinforcement of the structural overall stiffness

First, structural stiffening (SR) is proposed by diagonal tubular braces, connecting the top of the middle pile with the bottom of each lateral pile showed in Figure 8. Diagonal braces were modelled as link elements (BEAM188) with free rotation at ends (translational displacement fixed). Several diameter and thickness combinations of annular cross-section braces [identified by their axial stiffness (EA/L)] were studied. Maximum values of each studied variable were compared to those of the uncontrolled case (Figure 9). Since reinforcement of the structure was made by diagonal braces, a strong increase in support reactions at foundation level is expected. In order to reach the largest reduction in horizontal displacements with the lowest support reaction, stiffening should be a compromise between the two opposing targets.

Figure 8 Reinforcement of structural overall stiffness by means of diagonal braces

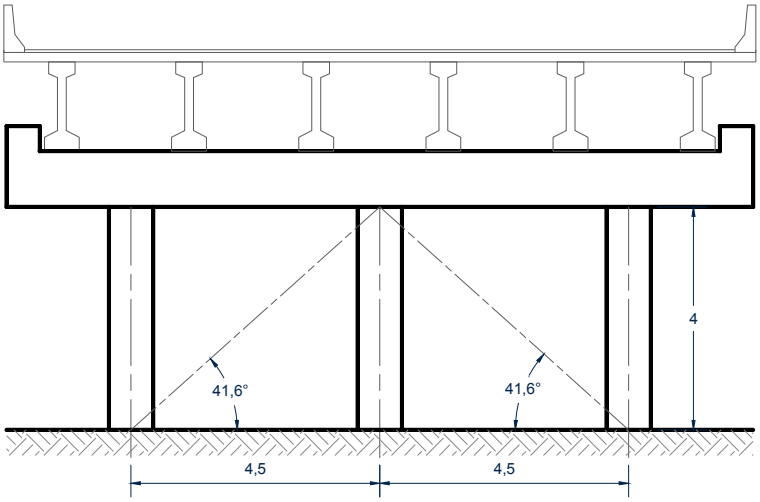

A circular cross-section with 230 mm diameter and 12.7 mm thickness is adopted, resulting in an axial stiffness of 350.3 kN/mm. This selection is based on the fact that maximum displacement observed does not decrease significantly with the increase in stiffness. With these assumptions, time history of structural response is shown in Figure 10, where uncontrolled response is also contrasted.

It is worth noting that the supports reaction is strongly increased despite the important reduction of displacements verified in all the studied cases. Thus, this solution is not considered feasible due to the need of reviewing a possible reinforcement in the foundation system in addition to the installation of the braces.

Moreover, it should be noted that the vertical support reaction reaches a negative value of –102 kN, which means lift in bearing connection. Nevertheless, this is a small amount of lifting that could be counteracted by the self-weight of foundation.

Figure 9 Maximum values associated with axial stiffness of diagonal brace, (a) horizontal displacement (b) horizontal displacements, amplified scale (c) horizontal component of support reaction (d) vertical component of support reaction (e) shear force in column

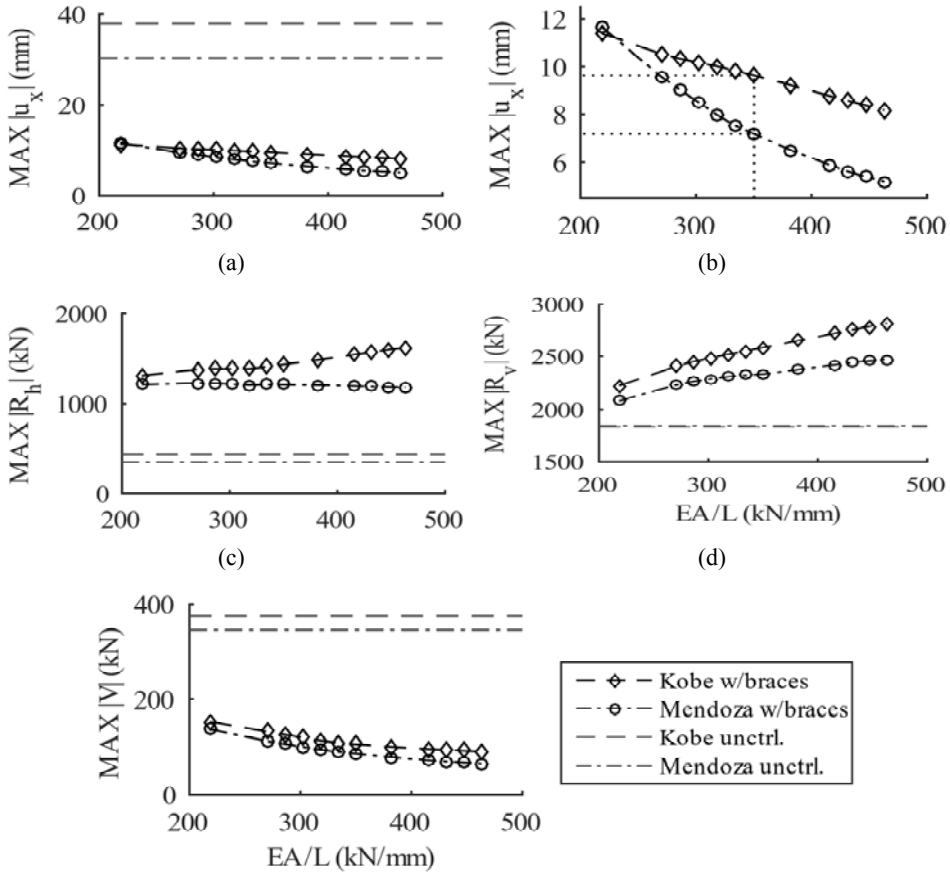

Figure 10 Time history of (a and b) horizontal displacement, (c and d) shear in column, (e and f) horizontal support reaction and (g and h) vertical support reaction of the structural stiffening

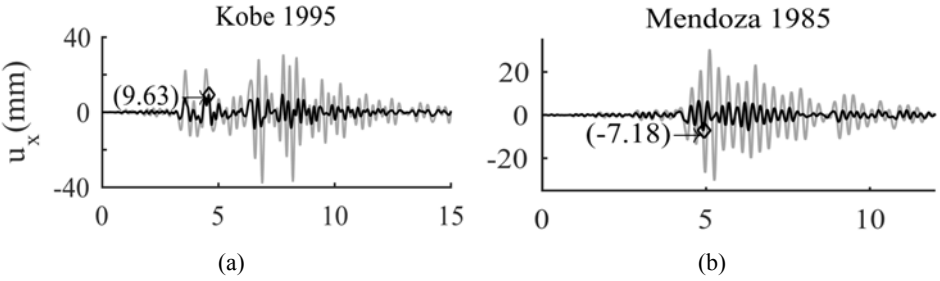

Figure 10 Time history of (a and b) horizontal displacement, (c and d) shear in column, (e and f) horizontal support reaction and (g and h) vertical support reaction of the structural stiffening (continued)

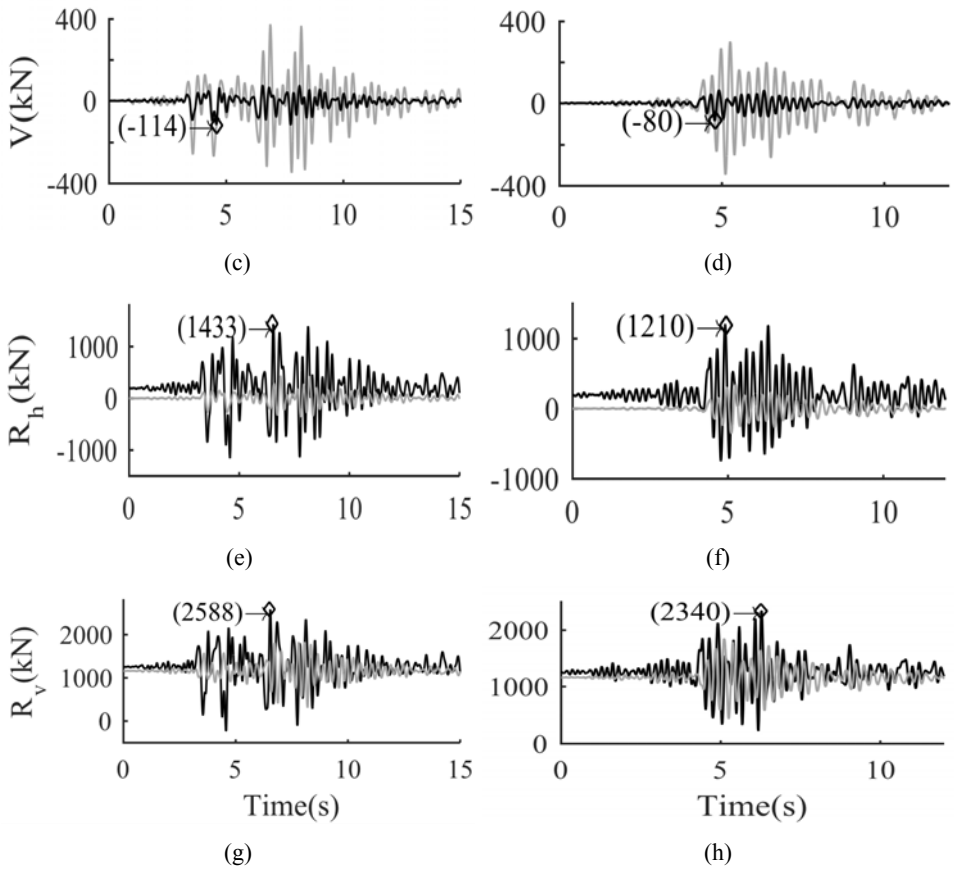

6.2 Tuned mass damper

This strategy, widely used in vibration control for high buildings, consists in attaching to the main structure a secondary vibration system (TMD), comprising a mass connected through a spring-dashpot, which dissipates part of input energy. These devices achieve large amounts of energy dissipated when their natural frequency of vibration coincides with the leading frequency of the vibrational mode that dominates the structural response.

The TMD is determined by three physical parameters that define its dynamic properties, they are mass (m), frequency of tuning (α) and damping (c). The mass quantity and damping coefficient of the TMD are usually expressed as a fraction of a known quantity. The ratio between device mass (m) and the mass of the first mode (M) is called μ and the damping ratio (ξ) is referred to the damping coefficient relative to the critical value (c_{cr}) [equation (1)].

$$\mu = \frac{m}{M}; \quad \alpha = \frac{\omega_{TMD}}{\omega}; \quad \xi = \frac{c}{c_{cr}} \tag{1}$$

There are several criteria to optimise those parameters according to different excitation types and scoped objectives (e.g., reduce the maximum displacements, base shear, etc.). In this paper, Warburton (1982) and Den Hartog (1956) criteria are used. The optimum parameters are presented in equations (2) and (3), respectively.

$$\alpha_{OPT} = \frac{\sqrt{1-\mu/2}}{1+\mu}; \quad \xi_{OPT} = \sqrt{\frac{\mu\left(1-\mu/4\right)}{4(1+\mu)\left(1-\mu/2\right)}} \tag{2}$$

$$\alpha_{OPT} = \frac{1}{1+\mu}; \quad \xi_{OPT} = \sqrt{\frac{3\mu}{8(1+\mu)^3}} \tag{3}$$

To represent the TMD in the original finite element model, a point mass (MASS21) was attached to the top of the middle column through a linear spring (COMBIN14), this element type includes the option of considering a viscous linear damper in parallel with a spring. The mass was allowed to move along the frame direction, parallel to the head girder that connects the top of the three piles. In this way, the TMD is tuned to the first mode, which is essentially a horizontal displacement along the direction of the middle frame plane.

Figure 11 Parametric evaluation of (a and b) maximum horizontal displacement and (c and d) RMS vs. mass ratio for Kobe and Mendoza earthquakes

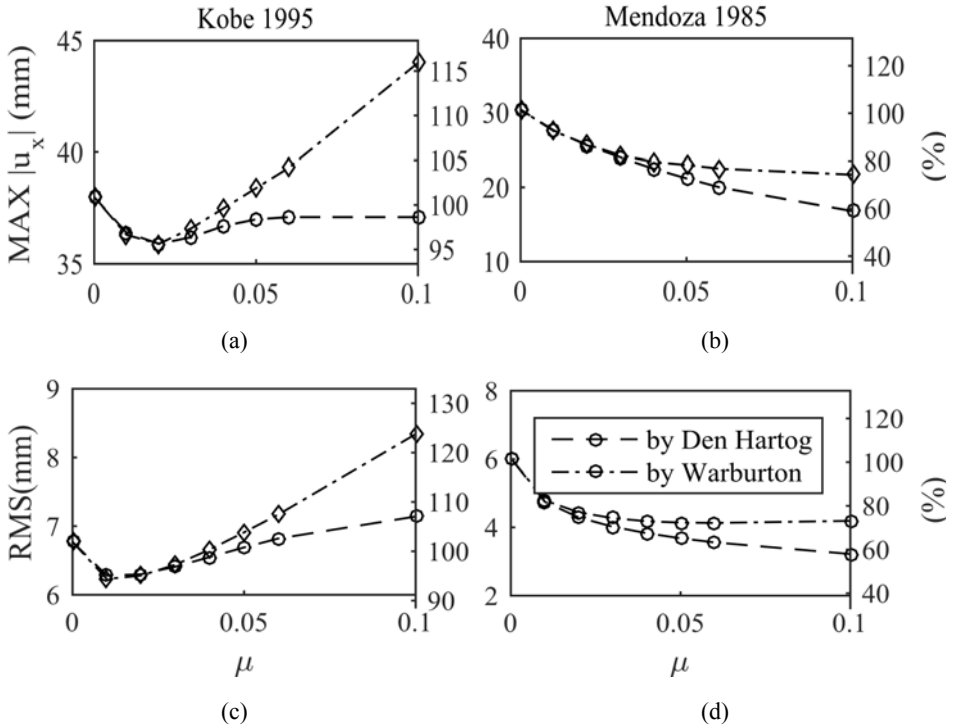

In order to optimally define TMD parameters, several different mass ratios were assessed. Both maximum and root mean square (RMS) values of horizontal time-history

displacements for each ratio are determined (Figure 11). A mass ratio of 0.02 is adopted due to the fact that both maximum displacement and RMS for Kobe earthquake are minimum. When the Mendoza earthquake is studied, these parameters decrease with a slower tendency.

Figure 12 Time history of (a and b) horizontal displacement, (c and d) shear in column, (e and f) horizontal support reaction and (g and h) vertical support reaction of the TMD alternative

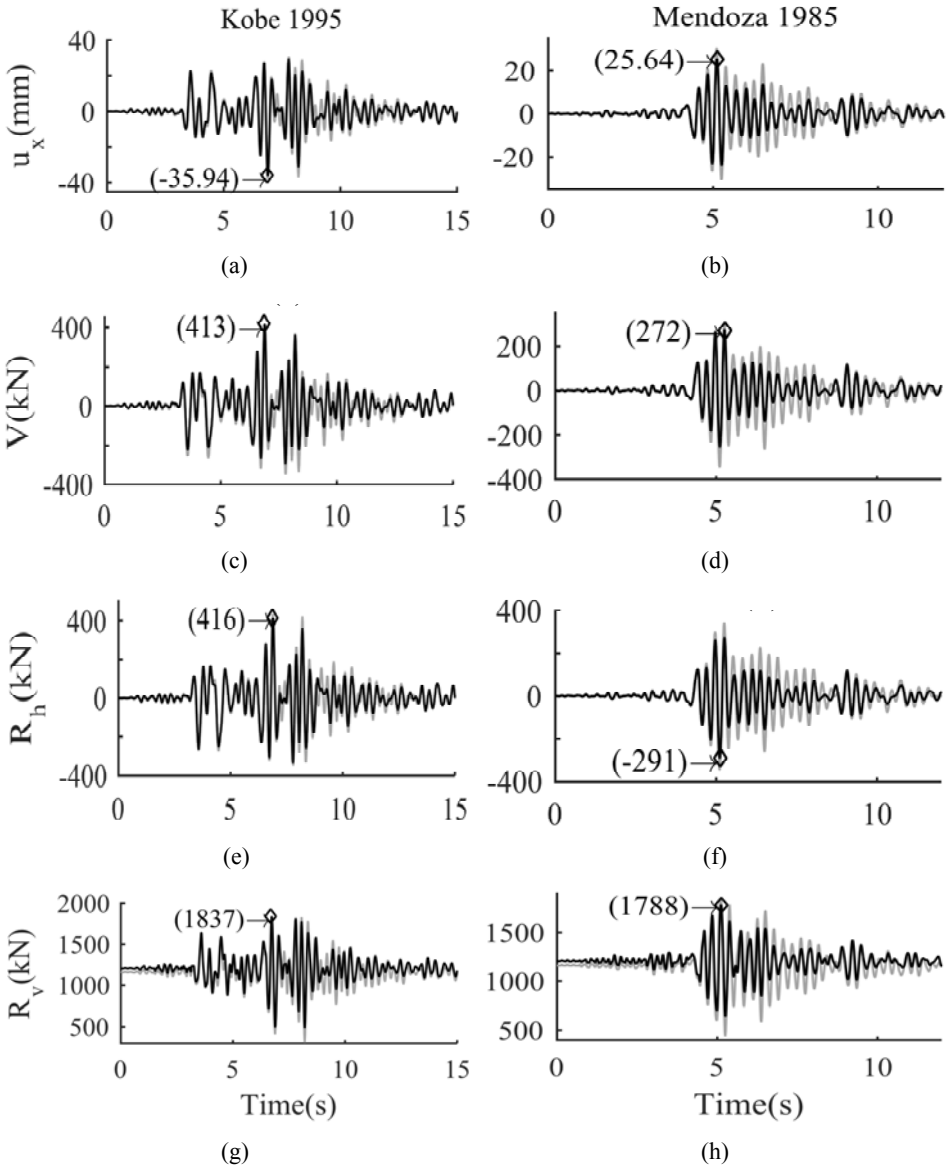

Despite the similitude of the results obtained by both criteria, the values proposed by Den Hartog (1956) equations were taken into account they imply minor values of stiffness and

damping coefficient in the damper. The time-history of structural responses are presented in Figure 12, where absolute maximum values are remarked.

6.3 Viscous fluid damper

In this alternative, two linear viscous fluid dampers (VFDs) with the same geometric configuration used in diagonal braces are installed. The dampers dissipate energy by forcing, through holes, the passage of a viscous liquid contained therein, turning the mechanical energy into heat that raises the temperature of the liquid (Martínez-Rodrigo and Filiatrault, 2015).

Figure 13 Maximum structural response vs. coefficient *C*

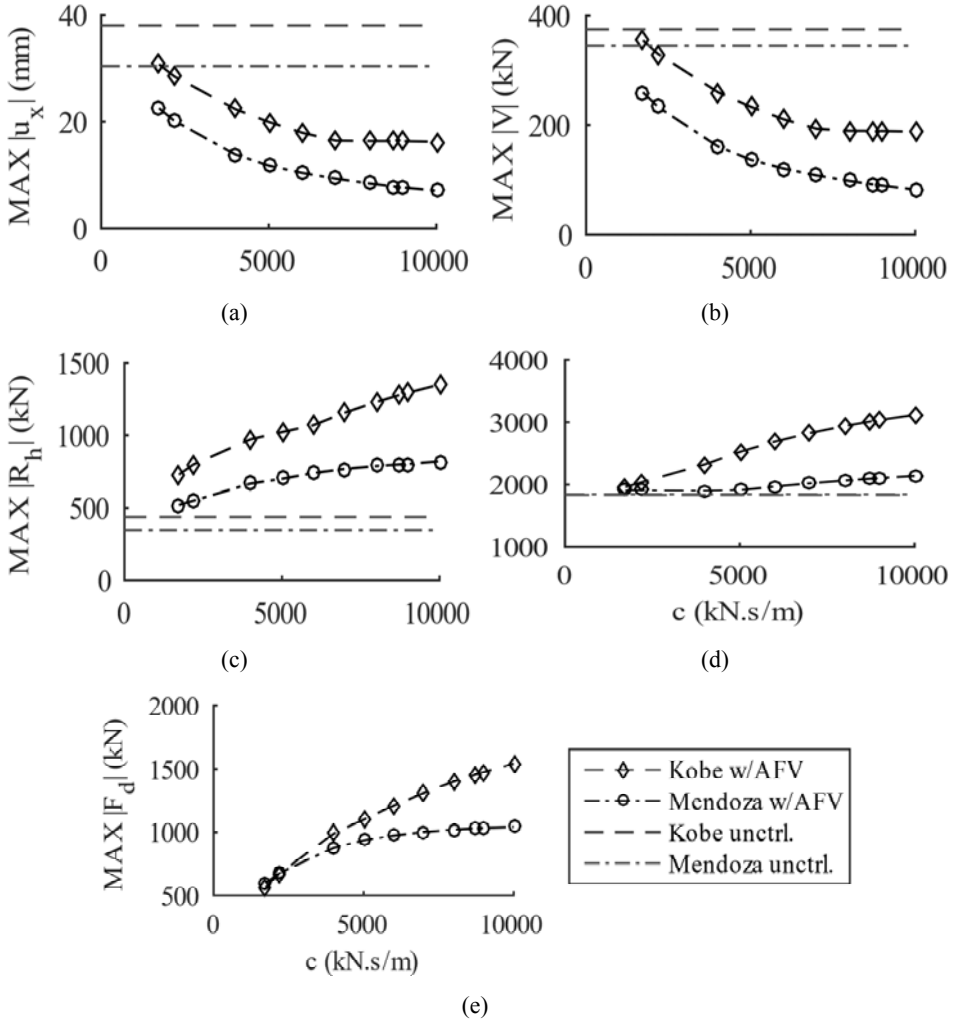

The linear VFD force is given by equation (4)

$$F_D = -C\dot{x} \tag{4}$$

in which C is damping coefficient and $\dot{x}$ is the relative velocity between extremes of the device.

Figure 14 Time history of (a and b) horizontal displacement, (c and d) shear in column, (e and f) horizontal support reaction and (g and h) vertical support reaction of the FVD solution

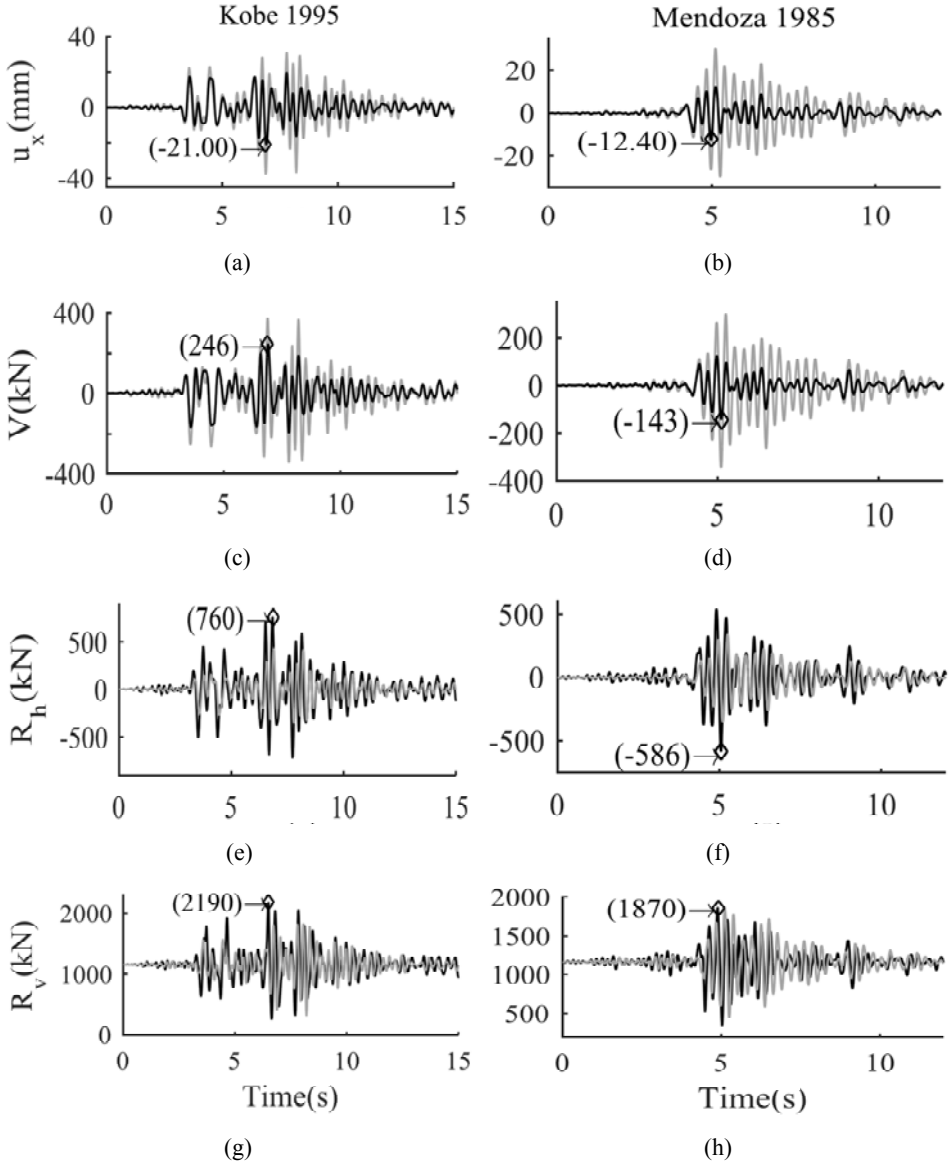

In order to select a suitable VFD for the studied case, the influence of the C coefficient on the dynamic response is evaluated (Figure 13). It is observed that as the value of C increases, there is a greater reduction of the maximum displacement, despite the increase support reaction. Finally, a coefficient of 4,000 kN.s/m is chosen for the VFD, due to the

fact that from this point onwards, the reduction observed in the maximum displacements becomes smaller. The structural response of the bridge with the adopted device is shown in Figure 14.

6.4 Metallic damper

Finally, a device with energy dissipation features based on the inelastic deformations of its metallic components, has been considered. MDs have been continuously developed since mid-1970s because they constitute one of the most effective mechanisms to dissipate energy given the stability of their hysteretic behaviour (Kumar et al., 2016). In this paper, an arrangement as indicated in Figure 15 is assumed. In relation to the model, MDs were introduced as a nonlinear spring with hysteretic behaviour (COMBIN39) whose force-displacement constitutive law is shown in Figure 15.

Figure 15 (a) Schematic arrangement of MDs into the bridge (b) Force-displacement constitutive law of the device

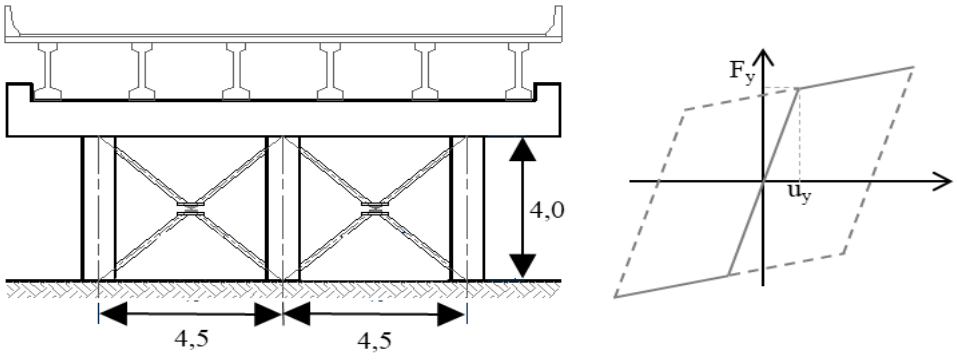

Figure 16 Variation of maximum values in studied parameters vs. yield of the MD

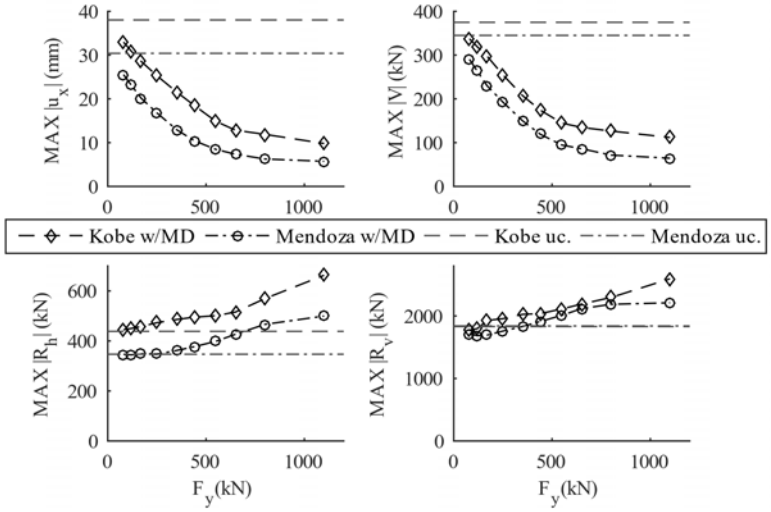

Figure 17 Time history of (a and b) horizontal displacement, (c and d) shear in column, (e and f) horizontal support reaction and (g and h) vertical support reaction of the bridge with MDs

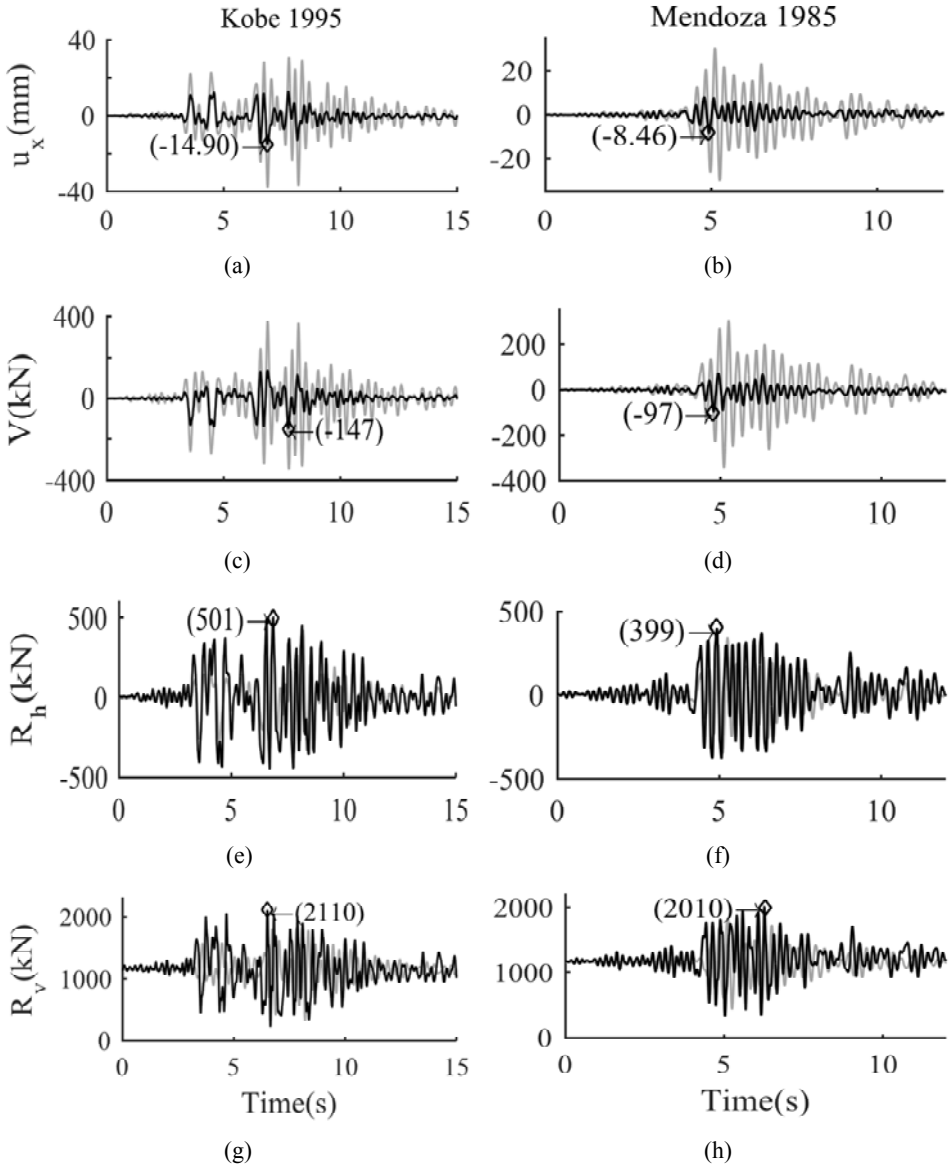

The features of the MDs are defined by their yield strength (F_y), yield displacement (u_y) and post-fluence stiffness. In this work, u_y is considered as a fix value and admitted equal to 20% of RMS value of the displacement uncontrolled response. Since the RMS value equals 6.77 mm and 6.03 mm, for the Kobe and Mendoza earthquakes, respectively, the yield displacement of the damper is set at 1.20 mm. In turn, post-fluence stiffness is established as 1.5% of elastic stiffness.

The yield strength is selected to be optimised through seismic performance. In this context, Figure 16 shows the maximum values of the studied parameters considering different F_y.

The criterion to establish the strength of the MD is based on obtaining a significant reduction of displacement (also in shear) without increasing considerably the support reaction. It should be noted that from 550 kN onwards, the reduction of maximum displacement is insignificant and at the same time, horizontal and vertical support reactions increase only about 15% (Figure 16). The dynamic performance of the bridge with adopted MDs is shown in Figure 17.

7 Discussions and conclusions

The maximum and RMS values of the studied parameters are presented in Table 4 for the Kobe earthquake and for the Mendoza earthquake in Table 5 for each suggested control system. Figure 18 displays these same results allowing direct comparison.

Table 4 Maximum values of studied parameters of the dynamic response in Kobe earthquake

Parameter	*Unit*	*Unctrl. (1)*	*SR (2)*	*TMD (3)*	*FVD (4)*	*MD (5)*
MAX $\|u_x\|$	(mm)	38.0	9.63	35.94	21	14.9
	(%)	*100%*	*25%*	*95%*	*55%*	*39%*
RMS $\|u_x\|$	(mm)	6.77	2.02	6.3	4.32	2.66
	(%)	*100%*	*30%*	*93%*	*64%*	*39%*
MAX $\|V\|$	(kN)	374.9	113.89	413.4	246	145.7
	(%)	*100%*	*30%*	*110%*	*66%*	*39%*
RMS $\|V\|$	(kN)	72.52	21.55	67.38	46.07	27.9
	(%)	*100%*	*30%*	*93%*	*64%*	*38%*
MAX $\|R_h\|$	(kN)	438.35	1433	415.96	760	501.3
	(%)	*100%*	*327%*	*95%*	*173%*	*114%*
RMS $\|R_h\|$	(kN)	77.62	345.04	72.42	142.8	128.3
	(%)	*100%*	*445%*	*93%*	*184%*	*165%*
MAX $\|R_v\|$	(kN)	1,813.3	2,587.8	1,837.2	2,190	2,112.4
	(%)	*100%*	*143%*	*101%*	*121%*	*116%*
RMS $\|R_v\|$	(kN)	1,170.7	1,287.5	1,213.9	1,176.8	1,158
	(%)	*100%*	*110%*	*104%*	*101%*	*99%*

The greatest reduction in maximum and RMS displacement is obtained by the classical stiffening of the structure (SR). Taking into account, the structural response under Kobe earthquake, it is possible to achieve a 75% reduction in the maximum displacement, in spite of a 227% increase in the horizontal support reaction. Regarding to Mendoza earthquake, this system provides a 76% reduction of maximum displacement reaching a 249% increase in the bearing force.

Figure 18 (a) Maximum and (b) RMS of displacement, (c) maximum and (d) RMS of shear in column, (e) maximum and (f) RMS of horizontal support reaction and (g) maximum and (h) RMS of vertical support reaction

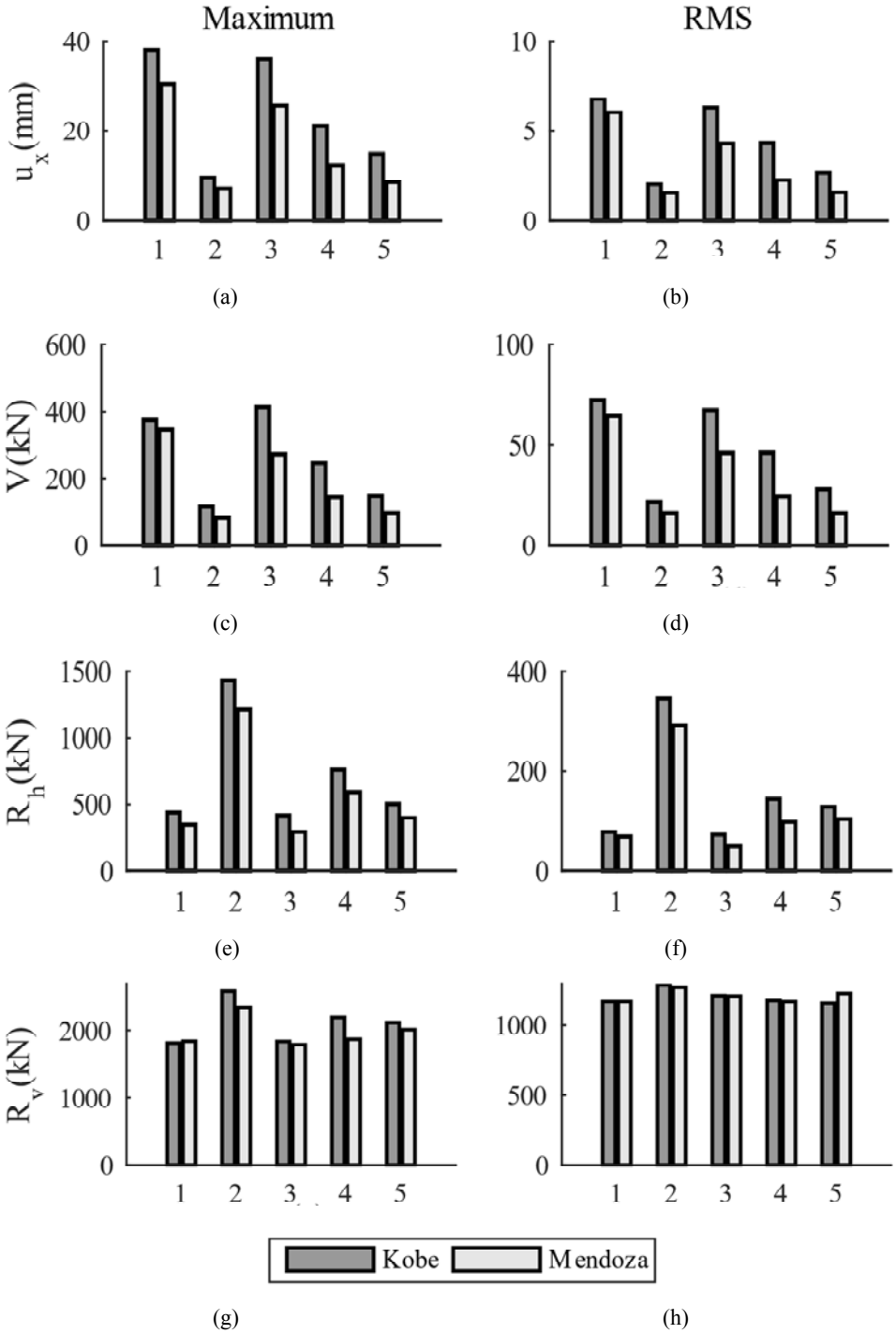

Table 5 Maximum values of studied variables in the Mendoza earthquake

Parameter	*Unit*	*Unctrl. (1)*	*SR (2)*	*TMD (3)*	*FVD (4)*	*MD (5)*
MAX $\|u_x\|$	(mm)	30.4	7.18	25.64	12.4	8.5
	(%)	*100%*	24%	84%	41%	28%
RMS $\|u_x\|$	(mm)	6.03	1.53	4.29	2.26	1.56
	(%)	*100%*	25%	71%	37%	26%
MAX $\|V\|$	(kN)	345	80.2	271.7	143	95.7
	(%)	*100%*	23%	79%	41%	28%
RMS $\|V\|$	(kN)	64.28	15.93	45.92	24.06	15.9
	(%)	*100%*	25%	71%	37%	25%
MAX $\|R_h\|$	(kN)	347	1210	291.13	586	398.7
	(%)	*100%*	349%	84%	169%	115%
RMS $\|R_h\|$	(kN)	68.47	290.74	48.72	97.6	103.9
	(%)	*100%*	425%	71%	143%	152%
MAX $\|R_v\|$	(kN)	1,840	2,340	1,787.5	1,870	2,009.7
	(%)	*100%*	127%	97%	102%	109%
RMS $\|R_v\|$	(kN)	1,170.8	1,273.3	1,211.6	1,169.9	1,229.6
	(%)	*100%*	109%	103%	100%	105%

On the other hand, the MDs has shown a slightly lower efficiency than SR, obtaining a 61% and a 72% reduction in the peak displacement reached in the Kobe and Mendoza earthquake respectively. Although in this case, the support reaction rises only 14% and 15%, respectively.

The VFDs appear as an intermediate solution, because these devices could achieve large reductions in the time-history of the displacements. Nevertheless, the support reactions could be strongly increased, though not as severely as in the case of the SR solution.

Finally, the alternative based on TMD shows the worst performance of the suggested systems, in terms of displacement reduction. These devices depend to a large extent on the tuning between excitation and device frequencies.

For all the above, it follows that MD is the best alternative suggested, achieving large reductions in horizontal displacements and columns shear force, while other structural parameters shown no significant increase.

Acknowledgements

The financial support of the CONICET and University of Cuyo is acknowledged. The technical documentation of the studied bridge supplied by Eng. Daniel Quiroga is also grateful. Special acknowledgements are extended to the reviewers of the first version of the paper because their useful suggestions led to improvements of the work.

References

Agrawal, A. et al. (2009) 'Benchmark structural control problem for a seismically excited highway bridge – part I: phase I problem definition', *Structural Control and Health Monitoring*, Vol. 16, No. 5, pp.509–529, DOI: 10.1002/stc.

ANSYS® (2010) Mechanical APDL Theory Reference, Release 17.0, Help System, ANSYS, Inc. Canonsburg, PA.

Beygi, H. (2015) *Vibration Control of a High-Speed Railway Bridge Using Multiple Tuned Mass Dampers*, Master thesis, KTH Royal Institute of Tecnology, Stockholm.

Clough, R.W. and Penzien, J. (2003) *Dynamics of Structures*, 3rd ed., Computer & Structures, Inc., Berkeley, CA, DOI: 10.1016/0045-7825(92)90174-I.

Den Hartog, J.P. (1956) *Mechanical of Vibrations*, McGraw-Hill Book Company Inc. New York, NY.

Domizio, M., Ambrosini, D. and Curadelli, O. (2015) 'Performance of tuned mass damper against structural collapse due to near fault earthquakes', *Journal of Sound and Vibration*, Vol. 336, pp.32–45, Elsevier, DOI: 10.1016/j.jsv.2014.10.007.

Han, Q. et al. (2009) 'Seismic damage of highway bridges during the 2008 Wenchuan earthquake', *Earthquake Engineering and Engineering Vibration*, Vol. 8, No. 2, pp.263–273, DOI: 10.1007/s11803-009-8162-0.

Housner, G.W. and Thiel Jr., C.C. (1995) 'The continuing challenge: report on the performance of state bridges in the Northridge earthquake', *Earthquake Spectra*, Vol. 11, No. 4, pp.607–636.

Hsu, Y.T. and Fu, C.C. (2004) 'Seismic effect on highway bridges in Chi Chi earthquake', *Journal of Performance of Constructed Facilities*, Vol. 18, No. 1, pp.47–53, DOI: 10.1061/(ASCE)0887-3828(2004)18:1(47).

Kawashima, K. and Unjoh, S. (1997) 'The damage of highway bridges in the 1995 Hyogo-Ken Nanbu Earthquake and its impact on Japanese seismic design', *Journal of Earthquake Engineering*, Vol. 1, No. 3, pp.505–541, DOI: 10.1080/13632469708962376.

Kawashima, K. et al. (2009) 'Damage of bridges in 2008 Wenchuan, China Earthquake', *Doboku Gakkai Ronbunshuu A*, Vol. 65, No. 3, pp.825–843, DOI: 10.2208/jsceja.65.825.

Kawashima, K. et al. (2011) 'Damage of Bridges due to the 2010 Maule, Chile, Earthquake', *Journal of Earthquake Engineering*, Vol. 15, No. 7, pp.1036–1068, DOI: 10.1080/13632469.2011.575531.

Kumar, P., Jangid, R.S. and Reddy, G.R. (2016) 'Comparative performance of passive devices for piping system under seismic excitation', *Nuclear Engineering and Design*, Vol. 298, pp.121–134, Elsevier B.V., DOI: 10.1016/j.nucengdes.2015.11.019.

Martínez-Rodrigo, M.D. and Filiatrault, A. (2015) 'A case study on the application of passive control and seismic isolation techniques to cable-stayed bridges: a comparative investigation through non-linear dynamic analyses', *Engineering Structures*, Vol. 99, pp.232–252, DOI: 10.1016/j.engstruct.2015.04.048.

Palermo, A., Liu, R., Rais, A., McHaffie, B., Pampanin, S., Gentile, R. ... and Wotherspoon, L.M. (2017) *Performance of Road Bridges during the 14 November 2016 Kaikoura Earthquake*.

Soong, T.T. and Dargush, G.F. (1997) *Passive Energy Dissipation Systems in Structural Engineering*, Wiley, Chichester, UK [online] http://www.wiley.com/WileyCDA/WileyTitle/productCd-0471968218.html.

Soria, J.M. et al. (2016) 'Exploring vibration control strategies for a footbridge with time-varying modal parameters', *Journal of Physics: Conference Series*, p.122170, IOP Publishing, DOI: 10.1088/1742-6596/744/1/012170.

Warburton, G.B. (1982) 'Optimum absorber parameters for various combinations of response and excitation parameters', *Earthquake Engineering & Structural Dynamics*, Vol. 10, No. 3, pp.381–401, DOI: 10.1002/eqe.4290100304.

Wotherspoon, L., Bradshaw, A., Green, R., Wood, C., Palermo, A., Cubrinovski, M. and Bradley, B. (2011) 'Performance of bridges during the 2010 Darfield and 2011 Christchurch earthquakes', *Seismological Research Letters*, Vol. 82, No. 6, pp.950–964.